ELSEVIER

Chemical Geology 226 (2006) 309–327

CHEMICAL GEOLOGY
INCLUDING
ISOTOPE GEOSCIENCE

www.elsevier.com/locate/chemgeo

^{4}He dating of groundwater associated with hydrocarbon reservoirs

Zheng Zhou [a,*], Chris J. Ballentine [b]

[a] Institute for Isotope Geology and Mineral Resources, ETH Zurich, NO C62.2, Sonneggstrasse 5, CH-8092 Zurich, Switzerland
[b] Department of Earth Sciences, The University of Manchester, Oxford Road, Manchester, M13 9PL, United Kingdom

Received 2 December 2004; received in revised form 1 April 2005; accepted 5 September 2005

Abstract

In this study, we show how physical models describing hydrocarbon/groundwater interaction can be developed by the noble gases in the hydrocarbon phase and, based on these models, initial crustal radiogenic ^{4}He concentrations in the associated groundwater can be calculated. Considering both in situ ^{4}He production and ^{4}He from an external crustal flux, this allows the ^{4}He age of the groundwater associated with each hydrocarbon reservoir to be derived. We illustrate the strengths and weaknesses of this approach using data from case studies from the San Juan Basin coalbed methane gas field in New Mexico, USA, the Magnus oilfield in the UK North Sea and the Hugoton-Panhandle giant gas field that spans Kansas, Texas and Oklahoma, USA.
© 2005 Elsevier B.V. All rights reserved.

Keywords: Noble gases; Groundwater; Dating; Hydrocarbon reservoirs; Oil; Gas

1. Introduction

Groundwater interaction with oil and natural gas plays a key role in hydrocarbon migration, filling and lifetime of a reservoir. On the basin scale the hydrodynamic system can physically control the secondary migration of oil and gas (e.g. Toth and Corbett, 1986; England et al., 1987; Ballentine et al., 1991). The interaction of water with the rock controls the creation or destruction of the porosity which in turn determines both the regional and reservoir aquifer quality (Summa, 1995; Ballentine et al., 1996; Lynch, 1996; Heydari, 2000), while extensive contact with groundwater can remove the most soluble phase through the process of 'water washing', degrading the quality of the reservoir hydrocarbons (Lafargue and Barker, 1988). Furthermore, groundwater can transport microbes to isolated or previously sterilized subsurface environments (Scott et al., 1994; Martini et al., 1996, 1998; Colwell et al., 1997; Tseng and Onstott, 1997; Walvoord et al., 1999) with resulting microbial biodegradation and alteration of oil and natural gas (Horstad et al., 1992; Rueter et al., 1994; Zengler et al., 1999). Understanding the timing however, remains a fundamental limiting factor in assessing when and on what time scale these processes have occurred.

At present there are a number of techniques available for dating groundwater. Assuming flow continuity, groundwater ages can be determined hydrologically based on Darcy's law, but remains of limited use when applied to old and deep basinal fluids (e.g. Ward and Robinson, 2000). The most common radiometric dating methods in groundwater research use the decay of cosmogenic or anthropogenic radioactive species to obtain ages, such as ^{14}C, ^{129}I and ^{36}Cl (Fontes and Garnier, 1979; Fabryka-Martin et al., 1987). However,

* Corresponding author. Tel.: +46 73 727 1334; fax: +41 1 632 1179.
E-mail addresses: zhou.eth@gmail.com (Z. Zhou), chris.ballentine@manchester.ac.uk (C.J. Ballentine).

0009-2541/$ - see front matter © 2005 Elsevier B.V. All rights reserved.
doi:10.1016/j.chemgeo.2005.09.030

these methods have their specific dating ranges, for example, ^{14}C ($T_{1/2}$=5730 years) can be used to date groundwaters up to 25,000–30,000 years old, with various correction required to account for the complexity of the local geology, hydrogeology and geochemistry (e.g. Fontes and Garnier, 1979).

Noble gases provide several important additional tracer systems that constrain groundwater residence, each encompassing a specific dating range (Kipfer et al., 2002). For example, ^{222}Rn ($T_{1/2}$=3.82 days) is suitable to trace groundwater processes that occur on a time scale of days (e.g. Hoehn and von Gunten, 1989). Anthropogenic radioisotope ^{85}Kr ($T_{1/2}$=10.76 years) and tritium decay to ^{3}He ($T_{1/2}$=12.32 year) can be used to date and identify young groundwater with ages up to about 60 years (e.g. Weise et al., 1992; Solomon et al., 1993). The cosmogenic radioisotope ^{39}Ar ($T_{1/2}$=269 years) dates the groundwater residence time between the ranges which can be dated by ^{14}C, ^{85}Kr and H–^{3}He (100–1000 years) (e.g. Loosli, 1983). In addition, the cosmogenic radioisotope ^{81}Kr ($T_{1/2}$=230,000 years) can be used to determine water residence times on time scales of 10^5 years, but because of technical demands remains highly specialised with only a limited number of case studies (e.g. Collon et al., 2000; Lehmann et al., 2003). On typical basinal fluid timescales, by far the most investigated groundwater dating tool remains the accumulation of stable radiogenic ^{4}He and ^{40}Ar in the groundwater, used for estimating groundwater residence on the Kyr to Myr timescales (e.g. Torgersen and Clarke, 1985; Torgersen and Ivey, 1985; Marty et al., 1993, 2003; Castro et al., 1998a,b; Osenbrück et al., 1998; Kipfer et al., 2002; Lehmann et al., 2003; Patriarche et al., 2004).

In this paper, we review how atmosphere-derived noble gases, originally dissolved in the groundwater, have been used to develop physical models to quantify gas/groundwater and oil/groundwater interaction. We show how these models allow us to compute the original ^{4}He in the groundwater phase associated with natural gas and oil reservoirs, and therefore enable a model ^{4}He age estimate of the hydrocarbon associated groundwater to be made. We use data and models from three existing studies to illustrate the application of this approach to very different mechanisms of hydrocarbon–water interaction: (1) The San Juan Basin coalbed methane gas field in New Mexico and Colorado, USA (Zhou et al., in press); (2) The Magnus oilfield, North Sea, UK (Ballentine et al., 1996); and (3). The Hugoton-Panhandle giant gas field in Kansas, Texas and Oklahoma, USA (Ballentine and Sherwood Lollar, 2002).

2. ^{4}He as a groundwater dating tool

2.1. ^{4}He in the groundwater

The accumulation of radiogenic ^{4}He in basin aquifers provides a suitable geochronometer for groundwaters because (1) the production of radiogenic ^{4}He is significant and easily identifiable from the natural atmospheric background and (2) the transfer of the ^{4}He from rock to fluid is fast on a geological time scale in most systems (Ballentine and Burnard, 2002). The use of this geochronometer requires the quantification of the accumulation rate of ^{4}He in groundwater. The amount of ^{4}He accumulated in a groundwater system can be expressed as:

$$[^4He] = [^4He]_{ASW} + [^4He]_{\text{in situ production}} + [^4He]_{\text{external flux}} \quad (1)$$

Where:

$[^4He]$ ^{4}He concentration in groundwater

$[^4He]_{ASW}$ Atmospheric ^{4}He concentration in air saturated water

$[^4He]_{\text{in situ production}}$ In situ crustal radiogenic ^{4}He concentration in the groundwater

$[^4He]_{\text{external flux}}$ ^{4}He concentration in the groundwater-derived from external sources.

$[^4He]_{ASW}$ is a function of temperature and pressure at groundwater recharge and fixed by the equilibrium solution of atmospheric ^{4}He. It is normally low due to the low He solubility in water and the low concentration of He in air. Both $[^4He]_{\text{in situ production}}$ and $[^4He]_{\text{external flux}}$ are functions of time and are described in details below.

2.2. In situ production and release of ^{4}He into the groundwater

^{4}He is produced in the crust by α decay of the $^{235,238}U$ and ^{232}Th decay chains. In situ ^{4}He concentration in the simplest system is then directly proportional to the concentrations of these radioelements in the crust, and time. There are several mechanisms responsible for the release of ^{4}He from minerals once it is produced, such as recoil loss, diffusive loss, fracturing loss and mineral breakdown caused by diagenesis, metamorphism or alteration (Torgersen, 1980; Ballentine and Burnard, 2002; Farley, 2002). The fractional release of He in the most common minerals can be assumed equal to unity for aquifer temperatures larger than 50–70 °C (Ballentine et al., 1994; Lippolt and Weigel, 1988).

The accumulation of in situ produced ^{4}He in the groundwater can be expressed as (Torgersen, 1980):

$$[^4\mathrm{He}]_{\text{in situ production}} = \frac{\rho \Lambda J_4 (1-\varphi)}{\varphi} t \quad (2)$$

Where:

ρ	Density of porous rock in g/cm^3
Λ	A parameter defining the efficiency of transfer from the rock matrix to groundwater
φ	Rock porosity
J_4	The source function of radioactive production of ^{4}He in the aquifer matrix in cm^3 STP ^{4}He/g_{rock} year
t	Groundwater residence time in year.

Assuming He loss from matrix minerals is fast on a geologic time scale (Ballentine and Burnard, 2002), Λ is considered to be close to 1 and J_4 can be expressed as (Craig and Lupton, 1976):

$$J_4 = 0.2355 \times 10^{-12} [U] \{1 + 0.123 ([\mathrm{Th}]/[U] - 4)\}. \quad (3)$$

Where: [U], [Th]=U and Th concentrations in rock in ppm.

This accumulated ^{4}He is valid assuming the detrital minerals in the matrix have not accumulated ^{4}He before sedimentation, or, it is released completely before sedimentation. In the case of young groundwaters, diffusion of inherited ^{4}He into the groundwater could become the dominant contribution of non-atmospheric helium (Solomon et al., 1996). But in the deeper and older groundwaters, the contribution of inherited ^{4}He trapped in the aquifer rocks are a minor component compared with other sources (Torgersen, 1980).

2.3. External flux of ^{4}He into the groundwater

Helium water age, computed assuming that radiogenic helium produced in the aquifer rock has been quantitatively transferred into the aquifer water, is often in excess of the ^{14}C age (Heaton, 1984), or the hydrologic age (Torgersen and Clarke, 1985). Indeed, there are many examples of groundwater systems that have concentrations of noble gases orders of magnitude higher than can be explained by local production, release and accumulation (e.g. Torgersen and Clarke, 1985; Takahata and Sano, 2000; Kipfer et al., 2002). This indicates that an external ^{4}He flux into groundwater is a common phenomenon. A large number of studies suggested that the origin of such ^{4}He "excess" is from the deep continental crust (e.g. Heaton, 1984; Andrews, 1985; Torgersen and Clarke, 1985; Stute et al., 1992; Marty et al., 1993; Castro et al., 1998a,b; Castro, 2004; Patriarche et al., 2004). Several studies also advocated that it is from intra-basinal sources such as old and stagnant waters, aquifer rocks and adjacent aquitard rocks (Tolstikhin et al., 1996; Pinti and Marty, 1998), or detrital minerals rich in inherited He and altered at low temperature (Torgersen, 1980; Solomon et al., 1996). These sources are probably contributing variable amounts of radiogenic He to deep aquifer waters, and their respective strengths can only be assessed by studies addressing well-documented aquifers.

A steady state crustal degassing model was developed to account for the high ^{4}He concentrations in the groundwater from the Great Artesian Basin, Australia (Torgersen and Clarke, 1985, 1987; Torgersen and Ivey, 1985; Torgersen, 1989; Torgersen et al., 1992; Bethke et al., 1999). This model requires the entire crustal volume to be releasing its radiogenic noble gases into the aquifer at the same rate as they are being produced. Similar 'steady state' rates have been inferred in other regional groundwater systems such as the Saijo Basin, Japan (Takahata and Sano, 2000), and the Paris Basin (Castro et al., 1998a,b), and from natural gas reservoirs (Sano et al., 1986). Estimates of ^{4}He flux into lakes can also be calculated with some showing similar values to the steady state reference, but with an order of magnitude variance (Kipfer et al., 2002). Both higher and lower fluxes than the average crustal degassing are observed elsewhere (Ballentine et al., 1991, 2002; Winckler et al., 1997; Kipfer et al., 2002). An explanation for this variance arises when we consider in more detail the environment in which ^{4}He is produced.

Since ^{4}He is not produced in sufficient quantities to form a continuous fluid capable of advective flow, it remains in trace quantities in the local pore fluids in the crust. The transport of the ^{4}He from the deep crust to near surface groundwater is dependant therefore on the behaviour of the fluid in the pore space. In a system that has no advective fluid flow, transport will occur by bulk diffusion, which in turn is controlled by the host rock characters such as permeability, tortuosity and the fluid occupying the pore space. When movement of fluid in the pore space occurs, these fluids will remove or carry the ^{4}He away from the site of release. However, a diffusive mechanism cannot account for significant noble gas mass transport from the deep crust, nor, given the permeability of the crust, is it reasonable that there is continuous and widespread fluid loss from the deep crust. The rate of external ^{4}He flux into groundwater is more strongly affected by large-scale tectonic events,

such as orogenesis and crustal extension (Ballentine and Burnard, 2002; Ballentine et al., 2002; Kipfer et al., 2002).

Nevertheless, because regional tectonic events resulting in metamorphism and ^{4}He release are common, the assumption that episodic release approximates steady state for old groundwaters provides a useful reference model. Based on the steady-state crustal degassing model, the external flux of ^{4}He into groundwater can then be expressed as:

$$[^4\mathrm{He}]_{\text{external flux}} = \frac{F_4}{\varphi h} t \quad (4)$$

Where:

φ	Rock porosity
h	Aquifer thickness in cm
t	Groundwater residence time in year
F_4	Average external crustal ^{4}He flux in cm^3 STP ^{4}He/cm$^2{}_{\text{rock}}$ year

F_4 can be calculated as:

$$F_4 = J_4 \cdot \rho \cdot H \quad (5)$$

Where:

ρ	Average crust density in g/cm^3
H	Average crust thickness in cm.

The external flux of ^{4}He into groundwater can also be from the mantle. This contribution is simply resolved using the different isotopic ratios of $^3\mathrm{He}/^4\mathrm{He}$ in the crust and mantle (Ballentine et al., 2002). Other uncertainties include the difficulties to obtain the porosity of the media, the grain size, the uranium and thorium concentrations in the solid phase, the inhomogeneities in uranium, thorium series elements and the release mechanism for ^{4}He from the solid phase. Probably the greatest of these uncertainties however, is the assumption that the steady state crustal degassing flux can be applied to all systems requiring an external flux. Case studies cited above clearly show up to an order of magnitude variation in this flux, and without local calibration (e.g. Castro et al., 1998b) or corroboration this does not a-priori enable a useful estimate of error on this variable to be made. In the absence of calibration, ^{4}He groundwater 'ages' only provide an indication of the groundwater age and, although relative dates will still be robust, absolute ages derived by this technique must be considered to be semi-quantitative. In systems where no other dating tool exists, this information is still able to provide critical insights into the timing of basinal fluid migration.

3. Case studies

3.1. Dating groundwater associated with San Juan Basin coalbed methane gas field, New Mexico/Colorado, USA

3.1.1. Geological background

The San Juan Basin, located across north-west New Mexico and south-west Colorado, USA, is currently one of the most prolific coalbed gas basins in the world (Fig. 1). The coal was deposited as peat during the Late Cretaceous. Localized post-coalification structural uplift occurred in the northernmost part of the basin, generating a structural hingeline. To the north of the hingeline, the coalbeds are highly fractured with resulting high hydraulic conductivity. To the south of hingeline the water permeability is low. The stratigraphy of the basin is characterized by alternating horizons of sandstones, limestones and shales of Cambrian to Tertiary age. Pictured Cliffs sandstones acted as platforms for Fruitland peat accumulation. The Fruitland formation is conformably overlain by the Kirtland shale throughout most of the basin (Scott et al., 1994). Meteoric water recharges the coalbed on the northwest basin margin. To the north of the structural hingeline is an artesian overpressured region, but the hingeline forms a barrier for water flow to the low permeability underpressured southern section. The gas production is high in the artesian overpressured area compared to the underpressured area due to enhanced biodegradation of the coal in this region (Scott et al., 1994).

Mavor et al. (1991) showed evidence of geological young groundwater in the Fruitland formation coalbed site with ^{14}C groundwater ages of around 33,000 years. Using 26 and 43 km flow paths from the north western and northern basin margins respectively, the residence times of Fruitland formation groundwater, calculated by Darcy's law, were approximately 15,000 and 28,000 years. However, a recent study of groundwater both in underpressured and overpressured areas of San Juan Basin coalbed gas field, using ^{129}I, ^{36}Cl and stable isotope of ^{18}O and D (Snyder et al., 2003), shows a contradictory result. A significant group of groundwater samples has $^{129}\mathrm{I}/\mathrm{I}$ ratios between 100×10^{-15} and 200×10^{-15}, indicating minimum iodine ages close to 60 Ma. If these ages are corrected for the addition of fissiogenic ^{129}I, they are compatible with the depositional age of the Fruitland formation (Late Cretaceous).

Phillips et al. (1986, 1989) and Stute et al. (1995) studied the aquifer overlying the Kirtland shale and Fruitland formation in the underpressured area of the San Juan Basin showing the groundwater ^{14}C ages in theses overlying aquifer to range from modern to 35,000 years.

3.1.2. Developing ^{4}He model groundwater ages

Noble gas studies of gas samples from coalbed methane gas producing wells in San Juan Basin gas field showed that the groundwater-derived noble gases in the produced gas phase can be used to develop a physical model to describe the gas/groundwater interaction (Zhou et al., in press). The model is based on the observation that both groundwater-derived noble gases (e.g. ^{20}Ne and ^{36}Ar) and resolved crustal radiogenic noble gases (e.g. ^{4}He and ^{40}Ar) are coherently fractionated, indicating that they are pre-mixed before fractionation occurs, probably in the groundwater phase. This then rules out the possibility that radiogenic gases associated with the gas phase alone, contribute to the system. Groundwater $^{20}Ne/^{36}Ar$, and crustal $^{4}He/^{40}Ar^{*}$ measured in the gas phase can both be modelled as open system gas loss from water following a Rayleigh fractionation process (Zhou et al., in press). We can use this model to compute the initial ^{4}He concentrations in the groundwater before degassing occurred. See Appendix 1 for detailed calculations. The initial crustal radiogenic ^{4}He concentrations in the groundwater associated with different gas producing wells are listed in Table 1.

If we take an average density of 1.79 g/cm^3 for the coalbed, U and Th concentrations 1.5 and 4.6 ppm, respectively (Finkelman et al., 1994), a porosity of 15% in the overpressured area and 3% in the underpressured

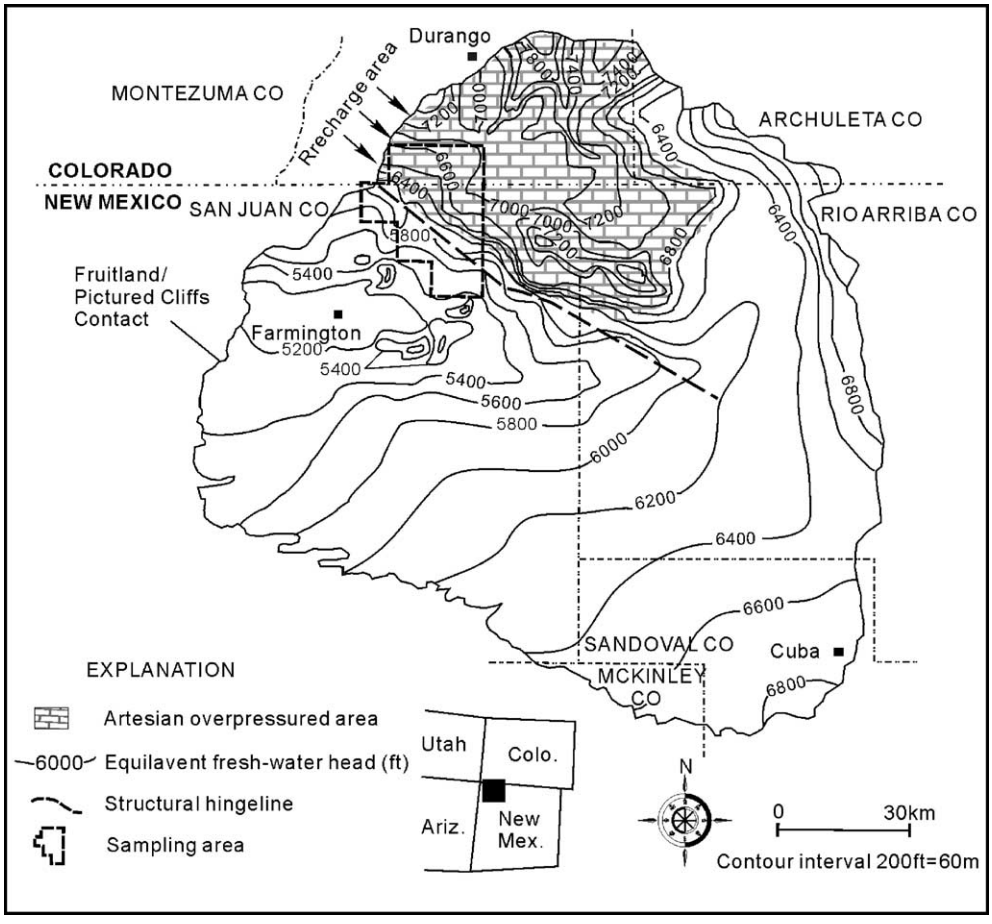

Fig. 1. Geological setting of the San Juan Basin and sampling area. It is located on the eastern margin of the Colorado Plateau, USA. The coal was deposited as peats during the Late Cretaceous. Localized post-coalification structural uplift caused a structural hingeline in the northernmost part of the basin. The coalbeds are highly fractured with high water permeability to the north of the hingeline, but to the south of hingeline the permeability of water is low. Meteoric water recharges the coalbed on the northwest basin margin. To the north of the structural hingeline is an artesian overpressured region, but the hingeline forms a barrier for water flow to the low permeability underpressured southern section (after Scott et al., 1994).

Table 1
Noble gas data from San Juan Basin, Magnus oilfield and Hugoton-Panhandle giant gas field

		Sample well	[^{4}He] (ppm) ($\times 10^{-2}$)	[^{20}Ne] (ppm) ($\times 10^{-5}$)	[^{36}Ar] (ppm) ($\times 10^{-2}$)	^{3}He/^{4}He (R/R_a) ($\times 10^{-2}$)	^{40}Ar/^{36}Ar	Resolved crustal radiogenic [^{4}He] (ppm) ($\times 10^{-2}$)	Initial [^{4}He] in groundwater (cm^3 STP/cm^3 H_2O) ($\times 10^{-3}$)	^{4}He ages[c] in closed system (year) ($\times 10^{+7}$)	^{4}He ages[c] in open system (year) ($\times 10^{+4}$)
San Juan Basin	Underpressured area	Decker100	634 (5)	161 (3)	62.204 (496)	9.87 (12)	385 (2)	625 (19)	1.96 (4)	10.79 (24)	3.83 (9)
		Culpepper Martin 103	4993 (54)	991 (24)	16.537 (99)	8.36 (23)	395 (1)	4930 (237)	1.19 (3)	6.56 (18)	2.33 (6)
		Culpepper Martin 109	8371 (91)	1323 (31)	16.416 (97)	10.07 (23)	394 (1)	8241 (366)	1.40 (4)	7.68 (21)	2.72 (7)
		Grenier101	10023 (109)	1089 (27)	8.998 (55)	12.29 (47)	428 (1)	9830 (536)	1.85 (5)	10.14 (28)	3.60 (10)
		Grenier103	11476 (124)	1344 (32)	11.426 (73)	11.71 (41)	421 (1)	11266 (584)	1.72 (5)	9.48 (26)	3.36 (9)
		Atlantic C 202	6226 (67)	261 (8)	2.277 (22)	14.93 (46)	541 (4)	6079 (343)	4.84 (17)	26.61 (94)	9.44 (33)
		King200	11592 (126)	411 (12)	2.930 (22)	16.79 (37)	625 (3)	11262(556)	5.46 (18)	29.99 (96)	10.64 (34)
		Sanchez2	5470 (59)	245 (7)	4.344 (30)	15.86 (35)	473 (2)	5332 (276)	5.37 (18)	29.48 (99)	10.45 (35)
	Overpressured area	Southern Ute 304	150.49 (86)	54.00 (90)	1.402 (9)	9.67 (9)	389 (1)	148 (4)	0.73 (1)	22.99 (45)	7.12 (14)
		Ute351	34.64 (20)	12.32 (40)	0.365 (2)	10.28 (9)	432 (1)	34 (2)	0.76 (3)	23.94 (81)	7.41 (25)
		Ute101	31.12 (34)	3.19 (10)	0.320 (2)	10.68 (9)	441 (1)	31 (1)	3.53 (12)	111 (4)	34 (1)
		Ute301	332.29 (2.74)	34.94 (54)	1.284 (7)	9.62 (8)	426 (1)	327 (9)	2.72 (5)	85 (2)	26.38 (50)
		Ute112	5.96 (7)	0.59 (7)	0.221 (1)	11.50 (14)	436 (1)	5.85 (97)	4.99 (59)	156 (18)	48 (6)
		Ute901	26.26 (29)	4.26 (8)	1.086 (7)	10.27 (7)	425 (1)	25.84 (83)	2.79 (6)	87 (2)	27.08 (61)
		Ute141	64.95 (71)	9.43 (25)	0.359 (2)	11.26 (9)	425 (1)	64 (3)	1.98 (6)	62 (2)	19.26 (57)
		Ute152	14.51 (16)	3.83 (27)	0.479 (3)	31.78 (23)	419 (1)	14 (1)	1.45 (10)	45 (3)	14 (1)
		Ute212	92.59 (67)	34.59 (91)	4.159 (21)	9.98 (8)	411 (1)	91 (4)	1.01 (3)	31.78 (89)	9.84 (28)
		Carter Ute 100	103.63 (59)	11.57 (15)	0.221 (2)	12.89 (10)	448 (2)	102 (2)	2.19 (4)	69 (1)	21.28 (38)
		Carter Ute 102	31.30 (18)	36.63 (1.00)	0.292 (2)	12.16 (9)	365 (1)	31 (1)	0.17 (1)	5.33 (16)	1.65 (5)
		Heizer100	29.65 (17)	4.19 (9)	0.212 (1)	12.64 (14)	442 (1)	29.06 (98)	2.18 (5)	68 (2)	21.18 (51)
		Burroughs Com A100	24.59 (14)	1.95 (9)	0.213 (1)	12.29 (12)	439 (1)	24 (2)	4.66 (21)	146 (7)	45 (2)
		Page Com 100	34.05 (19)	5.56 (17)	0.259 (2)	12.26 (12)	435 (2)	33 (2)	1.85 (6)	58 (2)	17.96 (59)
		Maddox Com 100	382.18 (2.17)	52.98 (1.62)	1.820 (12)	10.90 (8)	428 (1)	376 (17)	2.03 (7)	64 (2)	19.69 (64)
		Maddox Waller 101	841.22 (4.77)	76.99 (1.14)	1.857 (12)	11.01 (7)	433 (1)	827 (20)	2.83 (5)	89 (2)	27.43 (50)
		Primo Mudge100	41.98 (24)	4.40 (18)	0.299 (2)	13.07 (13)	430 (1)	41 (2)	3.15 (13)	99 (4)	31 (1)
		Ute121	4.43 (13)	1.39 (7)	0.125 (1)	11.80 (25)	444 (7)	4.35 (13)	1.12 (7)	35 (2)	10.91 (64)
		Ute161	40.8 (1)	15.2 (3)	3.99 (2)	10.00 (11)	418.0 (2)	40 (1)	1.22 (5)	38 (1)	11.81 (44)
		Ute132	4.75 (14)	0.597 (44)	0.129 (1)	13.30 (16)	442 (6)	4.65 (14)	3.47 (28)	109 (9)	34 (3)
		Ute202	217 (7)	50.6 (9)	5.19 (3)	10.00 (9)	415.0 (3)	214 (6)	1.57 (6)	49 (2)	15.23 (55)
		Ute242	25.7 (8)	2.34 (9)	0.426 (2)	12.10 (47)	435 (2)	25.24 (76)	4.59 (22)	144 (67)	45 (2)
		Ute231	112 (3)	15.4 (3)	0.500 (3)	10.50 (13)	433 (2)	111 (3)	2.02 (8)	63 (2)	19.64 (73)
		Ute401	94.5 (2.8)	26.9 (5)	2.08 (1)	9.53 (1)	423.0 (5)	93 (3)	1.20 (4)	38 (1)	11.64 (42)
		Southern Ute 300	70.1 (2.1)	16.3 (3)	0.563 (3)	9.42 (1)	427 (2)	69 (2)	1.21 (5)	38 (1)	11.79 (44)
		Stull100	42.3 (1.3)	5.96 (17)	0.233 (2)	12.20 (20)	447 (4)	41 (1)	2.06 (9)	64 (3)	19.96 (86)
		Maddox Mark 102	88.4 (2.7)	10.7 (2)	0.308 (2)	12.60 (16)	442 (4)	87 (3)	2.22 (8)	70 (3)	21.53 (81)
		Ute221	232 (7)	47.4 (9)	4.15 (2)	10.40 (19)	367.0 (3)	228 (7)	1.72 (6)	54 (2)	16.68 (60)

	Sample well	[^{4}He] (cm^3STP/cm^3) ($\times 10^{-2}$)	[^{20}Ne] (cm^3STP/cm^3) ($\times 10^{-6}$)	[^{36}Ar] (cm^3STP/cm^3) ($\times 10^{-5}$)	$^3He/^4He$ (R/R_a)	$^{40}Ar/^{36}Ar$	Resolved Crustal Radiogenic [^{4}He] (cm^3STP/cm^3) ($\times 10^{-2}$)	Initial [^{4}He] in groundwater (cm^3STP/cm^3H_2O) ($\times 10^{-3}$)	^{4}He ages[c] in closed system (year) ($\times 10^{+8}$)	^{4}He ages[c] in open system (year) ($\times 10^{+6}$)
Magnus Oilfield	A2	0.75 (14)	1.02 (23)	0.43 (15)	0.298 (15)	449 (6)	0.72 (14)	1.46 (58)	2.34 (94)	2.34 (94)
	A3	0.86 (18)	0.81 (9)	0.50 (15)	0.324 (6)	442 (5)	0.84 (19)	1.46 (54)	2.35 (86)	2.35 (86)
	A4	0.66 (12)	0.78 (8)	0.54 (14)	0.353 (7)	438 (4)	0.65 (12)	1.06 (33)	1.70 (54)	1.70 (54)
	A5	0.60 (11)	0.81 (9)	0.48 (13)	0.326 (7)	439 (8)	0.57 (12)	1.05 (36)	1.68 (58)	1.68 (58)
	A6	0.59 (9)	0.79 (8)	0.53 (13)	0.363 (7)	440 (3)	0.58 (9)	0.96 (28)	1.55 (45)	1.55 (45)
	B3	0.73 (13)	0.79 (9)	0.53 (14)	0.339 (7)	439 (5)	0.70 (13)	1.16 (38)	1.87 (61)	1.87 (61)
	B7	0.90 (18)	1.11 (24)	0.49 (16)	0.381 (19)	449 (12)	0.86 (18)	1.54 (61)	2.49 (99)	2.48 (99)
	D8	0.79 (14)	0.73 (7)	0.43 (11)	0.354(7)	443 (34)	0.76 (14)	1.53 (48)	2.46 (77)	2.46 (77)
Hugoton-Panhandle giant gas field	Hefner gas unit #1	0.397 (20)	0.1077 (75)		0.161	851 (11)		6.64 (57)	7.00 (60)	4.28 (37)
	Guldner unit #1	0.501 (25)	0.1556 (109)		0.139	835 (16)		5.80 (50)	6.11 (53)	3.74 (32)
	Guldner unit #2	0.427 (4)	0.1406 (12)		0.146	889 (5)		5.47 (7)	5.77 (7)	
	Keller, Ernest #2	0.379 (19)	0.0864 (60)		0.201	1066 (11)		7.90 (68)	8.33 (71)	5.10 (44)
	Jarvis unit #2	0.390 (20)	0.1067 (75)		0.200	1038 (20)		6.58 (57)	6.94 (60)	4.25 (37)
	Ball Clyde H. #2	0.352 (49)	0.1111 (11)			974 (47)		5.70 (9)	6.02 (9)	3.68 (6)
	Wright "C" unit #1	0.369 (4)	0.1187 (12)		0.183	948 (6)		5.60 (8)	5.90 (9)	3.61 (5)
	Baughman H-2	0.584 (6)	0.1798 (18)			977 (10)		5.85 (8)	6.17 (9)	3.77 (5)
	Crayton A-1	0.426 (21)	0.1188 (83)		0.193	969 (25)		6.45 (55)	6.81 (58)	4.17 (36)
	Mills C-1	0.376 (4)	0.1032 (10)		0.206	1155 (29)		6.56 (9)	6.92 (10)	4.23 (6)
	Parsely A-1	0.567 (28)	0.1232 (86)		0.208	925 (12)		8.28 (71)	8.74 (75)	5.35 (46)
	Oberly A-1	0.489 (25)	0.1613 (13)		0.192	830 (13)		5.46 (28)	5.76 (30)	3.52 (18)
	Tucker B-1	0.393 (29)	0.0993 (79)		0.188	967 (18)		7.12 (67)	7.51 (71)	4.60 (43)
	Barnes A-1	0.408 (4)	0.157 (16)			913 (18)		4.68 (48)	4.93 (51)	
	Buzzard D-1	0.454 (23)	0.1584 (111)		0.185	938 (26)		5.16 (45)	5.44 (47)	3.33 (29)
	Stonebraker A-69	0.646 (32)	0.2350 (164)		0.211	1113 (7)		4.95 (42)	5.22 (45)	3.19 (27)
	Coffee estate #1	0.636 (6)	0.1929 (19)		0.236	1156 (7)		5.93 (59)	6.26 (62)	3.83 (38)
	Blake Trust Estate#2	1.047 (52)	0.2923 (205)		0.246	1105 (25)		6.45 (55)	6.80 (58)	4.16 (36)
	Mary A Long #1	0.760 (38)	0.1980 (139)		0.204	1039 (17)		6.91 (60)	7.29 (63)	4.46 (38)
	Donelson et al. #1	0.983 (49)	0.5032 (352)		0.208	1076 (7)		3.52 (30)	3.71 (32)	2.27 (20)
	Sarah Claybaugh #1	0.923 (46)	0.4958 (347)		0.183	865 (33)		3.35 (29)	3.53 (30)	2.16 (19)
	Cameron Walls #1	0.661 (33)	0.1752 (122)		0.202	1112 (15)		6.79 (58)	7.16 (61)	4.38 (38)
	Horner #1	0.917 (9)	0.3687 (31)		0.184	1058 (14)		4.48 (6)	4.72 (6)	2.89 (4)
	Whitherbee #2	0.350 (18)	0.0821 (57)		0.212	983 (11)		7.67 (66)	8.09 (70)	4.95 (43)
	Flores 23	0.607 (6)	0.1753 (18)			1118 (12)		6.23 (9)	6.57 (9)	4.02 (6)
	Nisbett #1	0.547 (27)	0.1522 (107)		0.190	1045 (9)		6.47 (56)	6.82 (59)	4.18 (36)
	Air[a]	0.000524	16.5	3.12	1	295.5				
	ASW[b]	0.0000045	0.17	0.11						

1 sigma errors are shown as last significant figures in parentheses.

[a] Ozima and Podosek (1983).

[b] Noble gas concentrations in air-saturated water (ASW) were calculated following Henry's Law corrected for an altitude of 600 m, a recharge temperature of 10 °C and an unfractionated excess air component assuming 15% excess air Ne (e.g. Kipfer et al., 2002; Stute et al., 1992, 1995).

[c] Errors for ^{4}He ages only include the propagated errors of measured ^{4}He in the calculation.

Table 2
^{4}He accumulation rates in the groundwater and the parameters used for calculation

		[U] (ppm)	[Th] (ppm)	Th/U	Density (g/cm^3)	Porosity (%)	Thickness	Accumulation rate (in situ) (cm^3 STP ^{4}He/cm ^{3}H$_2$O year)	Accumulation rate (external) (cm^3 STP ^{4}He/cm^3 H$_2$O year)
San Juan Basin	Underpressured area	1.5	4.6	3.1	1.79	3	15 m	1.82×10^{-11}	5.13×10^{-8}
	Overpressured area	1.5	4.6	3.1	1.79	15	15 m	3.19×10^{-12}	1.03×10^{-8}
Magnus		4.8	7.6	1.6	2.6	25	150 m	6.21×10^{-12}	6.16×10^{-10}
Hugoton-Panhandle		2.8	10.7	3.8	2.6	15	100 m	9.48×10^{-12}	1.54×10^{-9}
Average crust	Upper	2.8	10.7	3.8	2.6	–	10 km		
	Lower	0.28	1.07	3.8	3.3	–	30 km		

area (Stone et al., 1983) (Table 2), the accumulation of ^{4}He in the groundwater by in situ production can be calculated following Eqs. (2) and (3). This gives an accumulation rate of 1.82×10^{-11} cm^3 STP ^{4}He/cm^3 H$_2$O year in the underpressured area and 3.19×10^{-12} cm^3 STP ^{4}He/cm^{3}H$_2$O year in the overpressured area.

In a closed system, the ^{4}He concentration in the groundwater is only a function of the ^{4}He accumulation by in situ ^{4}He production. The calculated ^{4}He groundwater ages from this relationship are between 6.56×10^7 to 3.00×10^8 years in the underpressured area and between 5.33×10^7 to 1.56×10^9 years in the overpressured area (Table 1). These dates are clearly not valid because they are even older than the age of the deposition of the coalbed, and therefore demand an external ^{4}He flux.

^{3}He/^{4}He ratios higher than average crustal production ($0.007R_a$) in San Juan gas samples ($0.08R_a$–$0.3R_a$) indicate a resolvable magmatic component (Zhou et al., in press). This also requires a flux from beneath of the basin. Therefore, it has to be expected that radiogenic ^{4}He is transported into the aquifer from the deep crust by advection, diffusion and/or dispersion. We use the model developed by Torgersen and Ivey (1985) to account for the external flux of ^{4}He into an open groundwater system. The accumulation due to an external ^{4}He flux into groundwater can be calculated using Eqs. (4) and (5). The parameters used for average crust composition (Taylor and McLennan, 1985) are listed in Table 2 to give an average total crustal ^{4}He flux of 2.31×10^6 cm^3 STP ^{4}He/cm^2 year. Porosities for the San Juan Basin coalbed are the same as described above. In addition we need to know the aquifer thickness (e.g. Eq. (4)). For both over- and underpressured regions the San Juan coalbed average is 15 m (Table 2). The calculated ^{4}He accumulation rates from an external flux into the groundwater are then 5.13×10^{-8} cm^3 STP ^{4}He/g H$_2$O year in the underpressured area and 1.03×10^{-8} cm^3 STP ^{4}He/g H$_2$O year in the overpressured area. The difference of the accumulation rate between underpressured area and overpressured area is dominated by the difference in porosity between the two systems. The accumulation of an external ^{4}He flux into groundwater is much larger than the accumulation of ^{4}He produced in situ.

Taking both the in situ ^{4}He accumulation and the ^{4}He accumulation from the external flux into account, we calculate groundwater ages to be between 2.33×10^4 and 1.06×10^5 years in the underpressured area and between 1.65×10^4 and 4.84×10^5 years in the overpressured area (Fig. 2). In the underpressured area, groundwater ages increase (solid line) as a function of the distance from basin margin recharge area. In the overpressured area, groundwater dates are scattered and while there may be

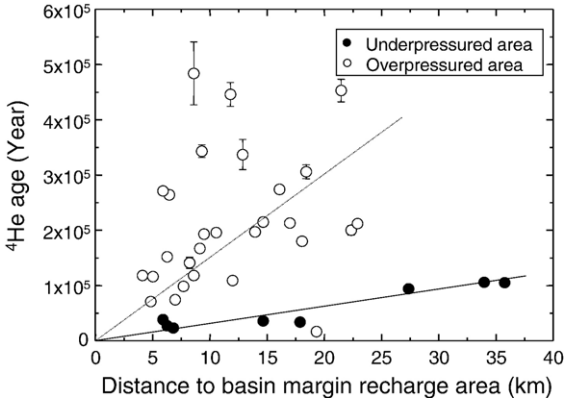

Fig. 2. ^{4}He ages of groundwater associated with coalbed methane producing wells in San Juan Basin, USA (Errors only include the uncertainties of ^{4}He in the measurements and calculation of initial ^{4}He in the groundwater). These ages were calculated assuming the accumulation of crustal radiogenic ^{4}He in the groundwater is from both in situ production and an external flux by steady-state crustal degassing (see text). In the underpressured area, groundwater ages are increasing as a function of the distance to basin margin recharge area, but there is no clear spatial trend of groundwater ages in overpressured area. Groundwater ages in the underpressured area are significantly younger than those in the overpressured area. This is probably because the structural hingeline forms barrier for water following in the overpressured area, but in the underpressured are, there is not such a restriction.

a tendency to increase with increasing distance to recharge (dashed line) there is no clear trend. For all of the overpressured samples, correction for the Rayleigh fractionation degassing of the groundwater system is far higher than for the underpressured samples (Zhou et al., in press). Small deviations from the simple degassing model will propagate uncertainty in the derived ^{4}He concentration of the water and probably accounts for the higher degree of scatter in resolved model ^{4}He groundwater ages for the overpressured portion of the aquifer. Groundwater ages in the underpressured area are nevertheless significantly younger than those in the overpressured area. This is entirely consistent with a simple hydrogeological model in which the structural hingeline forms a barrier for water flowing in the overpressured area, but with no such restriction in the underpressured area.

3.1.3. San Juan Basin—summary

The ^{4}He groundwater ages we obtained assuming open and closed systems are 3–4 orders of magnitudes different from each other. This is because in an open system, the crustal degassing of ^{4}He into the groundwater is the dominant ^{4}He accumulation mechanism. The dates obtained from 1.65×10^4 to 4.84×10^5 are the estimates of the ages of groundwater involved in the San Juan Basin gas production. As we discussed before, the choice of physical parameters can affect the relative ^{4}He dates resolved, with the key variables being aquifer thickness, porosity and U, Th concentrations, while the assumption of an average crust ^{4}He flux clearly affects the absolute dates obtained for the system.

The difference in model ^{4}He age between the two different regions does appear to have a reasonable physical basis. The abrupt increase in porosity at the basin hingeline has clearly had a major impact on groundwater flow through the high production Fruitland coal, evidenced by the artesian overpressure of the associated groundwater. A model in which continuous recharge of the Fruitland formation occurs at outcrop will result in the high porosity system reaching saturation and causing artesian overspressuring because of the limited leakage caused by the porosity decease at the basin hingeline. Water in the high porosity system is then expected to be older than water in the low porosity and underpressured region, where what limited recharge occurs is restricted to limited flow pathways, and has no confinement, enabling continued recharge and flushing of the system. It is nevertheless impossible to rule out an increased ^{4}He flux into the overpressured region caused by enhanced fracturing of the uplifted portion of the basin being the cause of the relatively older ages in this portion of the basin. While any spatial information appears to have been lost in the noise of the overpressured San Juan gases, the clear increase in age with increasing distance from basin margin of the underpressured gases provided confidence in the interpretation of relative age in any one portion of the basin, as this is far less subject to uncertainty in the ^{4}He flux rate.

The ^{4}He groundwater dates in the centre of the underpressured area using average crustal flux rates are consistent with ages of major recharge events (22,000 years BP) reported for the San Juan Basin (Phillips et al., 1986). These dates also agree with the ^{14}C dates and are close to the hydrological modelling dates up to the distance of 20 km from the basin margin recharge area (Mavor et al., 1991) (Fig. 2). Our results do not support the groundwater ages of ~60 Ma reported by (Snyder et al., 2003) in any sense or form. This result is critical in understanding the timescale required to generate the significant/commercial quantities of biogenic gas from the overpressured Fruitland coal formation. If the system has been open to fluid flow prior to closure and establishing the artesian overpressure, suggested by our data and model age, no significant build up of gas would be expected prior to overpressuring. The work presented here then places an upper limit on the time required to generate these volumes of biogenic methane on the order of tens of thousands of years.

3.2. Dating groundwater associated with Magnus oilfield, North Sea, UK

3.2.1. Geological background

The Magnus oilfield is located in the Brent Province of the UK North Sea (Fig. 3). The field consists of a single oil phase with no associated gas cap. Hydrocarbon accumulations within the Brent Province occur in Middle Jurassic sandstones located on the dipping flanks of tilted Jurassic fault blocks which were active both prior to and after deposition of the reservoir sandstones. The Magnus Sandstone is Kimmeridgian in age and was deposited in lobes from a submarine fan system. The lithology is a fine- to medium-grained arkosic sandstone with an in-reservoir porosity which varies between 20% and 27% (Emery et al., 1993).

3.2.2. Developing ^{4}He model groundwater ages

Ballentine et al. (1996) argued that the atmosphere-derived ^{20}Ne and ^{36}Ar in the Magnus oil have been due to noble gas partitioning between a seawater-derived groundwater and the oil phase. An oil and water volume ratio for the Magnus system of $V_{oil}/V_{water}=0.009\pm0.003$ was defined by the magnitude of ^{20}Ne/^{36}Ar

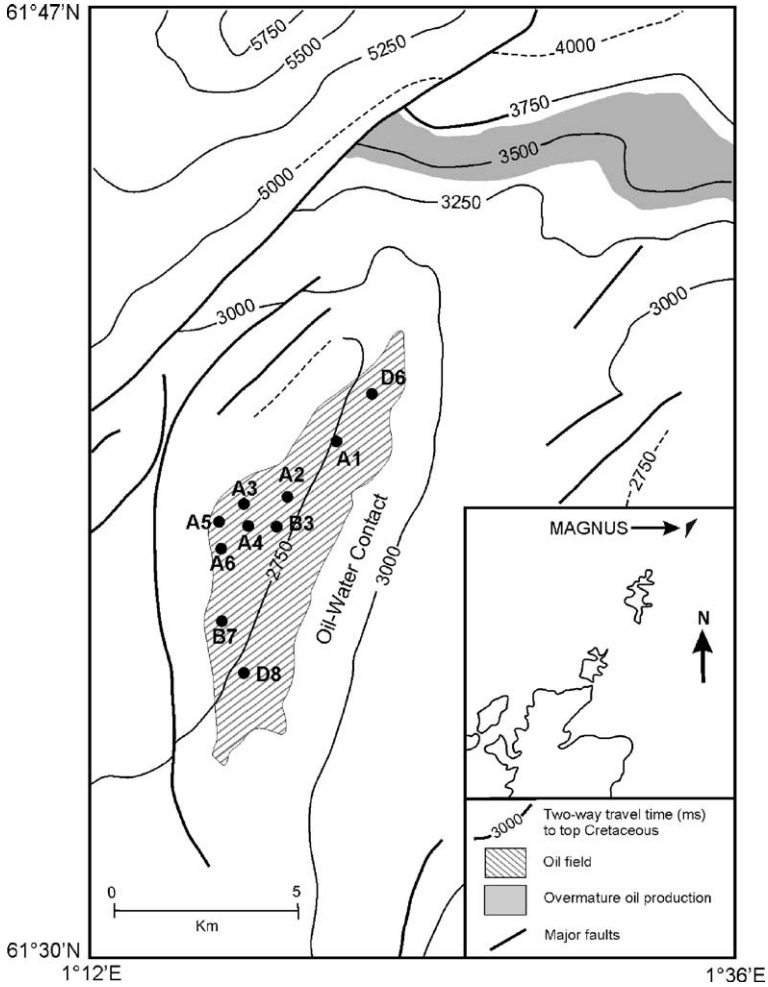

Fig. 3. Geological setting and sample details of Magnus oilfield. It is located in the Brent Province of the UK North Sea. The major faults are shown together with isopaches to the base Cretaceous (after Ballentine et al., 1996).

fractionation from seawater values observed in the Magnus oil phase. The ratio of radiogenic noble gases to seawater-derived noble gases in the system is near constant and it is reasonable to assume that the radiogenic noble gases would also be partitioned between the groundwater and oil phase. Because we know the ^{4}He concentration in the oil phase, the oil/water volume ratio and have reasonable estimates of the temperature and salinity conditions under which partitioning occurred (Ballentine et al., 1996), it is possible to calculate the initial ^{4}He concentrations in the groundwater. We present the detailed calculations in Appendix 2. The initial crustal radiogenic ^{4}He concentrations in the groundwater associated with Magnus oil wells are listed in Table 1.

Radioelement concentrations and porosities have been determined for the Magnus reservoir (Ballentine et al., 1996). We took the average reservoir U concentration of 4.8 ppm, Th concentration of 7.6 ppm for the calculation of ^{4}He produced in situ. The average porosity is taken to be 25% and the density is taken as the average crust value of 2.6 g/cm^3 (Table 2). Using Eqs. (2) and (3), the calculated crustal radiogenic ^{4}He concentration accumulated in the groundwater by in situ production is 6.21×10^{-12} cm^3 STP ^{4}He/cm^3 H_2O year.

Assuming a closed system, the combination of initial ^{4}He concentration in the groundwater and the accumulation rate of ^{4}He in the groundwater by in situ production gives the in situ production model ages of the groundwater associated with the oilfield. They range between 1.55×10^8 years and 2.49×10^8 years (Table 1). Closed system calculations are clearly nonsensical as these dates are even older than the deposition of the reservoir rocks. This shows that the volume of rock required to produce the radiogenic noble gases within

the Magnus reservoir cannot be accounted for by in situ production. Production from outside the Magnus sandstone formation must therefore provide the predominant portion of the radiogenic noble gases. The observation that, in the same way as in the San Juan system, mantle-derived noble gases are also observed in the Magnus field provides strong evidence for cross-formational communication with deeper regions of the crust (Ballentine et al., 1996).

We use here again the steady-state crustal degassing model developed by Torgersen and Clarke (1985) to estimate the external ^{4}He flux into the groundwater associated with the Magnus oilfield. All parameters are the same as the average crust values used in San Juan Basin study, but the aquifer thickness and porosity use average reservoir values of 150 m and 25%, respectively (Table 2). Taking an average crustal ^{4}He flux of 2.31×10^6 cm^3 STP ^{4}He/cm^2 year, the ^{4}He accumulation rate in the groundwater can be calculated following Eq. (4). In an open system, the total ^{4}He accumulation in the groundwater is the sum of the accumulation rate by in situ production and the accumulation rate by external flux. The ^{4}He accumulation rate in the groundwater associated with Magnus oilfield is 6.22×10^{-10} cm^3 STP ^{4}He/cm^3 H_2O year and dominated by the external flux. The ^{4}He concentration in the groundwater associated with the Magnus oil is then accounted for by model groundwater ages of between 1.55×10^6 and 2.48×10^6 years (Table 1; Fig. 4). Considering the error propagation in the calculation of initial ^{4}He concentrations in the groundwater, which is up to 40% of the calculated values, these dates are within error of each other and there is no resolvable spatial trend of groundwater age preserved in Magnus oilfield.

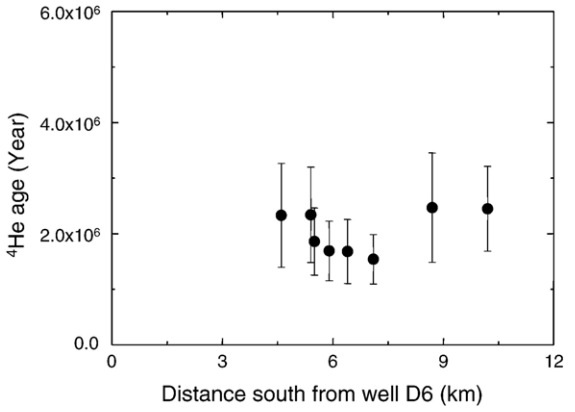

Fig. 4. ^{4}He ages of groundwater associated with Magnus oilfield, UK (Errors only include the uncertainties of ^{4}He in the measurements and calculation of initial ^{4}He in the groundwater). There is no clear spatial trend of groundwater ages in the Magnus oilfield. These dates suggest that there is no significant preservation of formation water in the Magnus oil reservoir. The aquifer system, even after the hydrocarbon sealing formation is in place, is active and replenished (see text for discussion).

3.2.3. Magnus oilfield—summary

These model groundwater age of ~2 Myr can be put into context by considering the timing of the major Magnus field geological events: I) 150 Ma since sedimentation of the Magnus sandstone; II) 90 Ma since the formation of the trapping structure; and III) reservoir filling and permeability loss at the oil/water interface between 62 and 72 Ma (Emery et al., 1993), closing the system. Because of permeability decrease due to quartz cementation during oil filling, the model ^{4}He groundwater ages most reasonably reflects the age of the groundwater contacted by the oil during filling. While there is a small amount of scatter in excess of analytical uncertainty, there is no clear spatial trend. As a starting point we simply consider the average model ^{4}He groundwater age of ~2 Myr. This compares with the average time between trap formation and reservoir filling of ~25 Ma, and between trap filling and sedimentation of 85 Ma. Even given the many uncertainties in obtaining absolute ages using the ^{4}He groundwater technique, it is clear that the oil has not contacted water trapped during the sedimentation of the Magnus sandstone ('formation water'). It is also highly unlikely that the water present in the Magnus sandstone aquifer when the seal was formed was the water contacted by the oil during migration from source rock to trap. Only the duration over which time filling is estimated to have occurred, of some 10 Myr, starts to approach the model ^{4}He groundwater age we have derived.

This work then provides a unique picture of the groundwater environment in a major oil producing system. There is no significant preservation of 'formation' water. The aquifer system, even after the hydrocarbon sealing formation is in place, is active and replenished. On the timescale of, or as a consequence of oil charging (with concurrent cementation of the Magnus Sandstone at the oil/water contact), any groundwater flow through the Magnus aquifer is however limited. A constraint on the water flux through the system during oil charging is the total volume of groundwater that the Magnus oil has equilibrated with. This can be accounted for by the static volume of water within the Magnus sandstone aquifer (Ballentine et al., 1996). This limited volume of water that has contact the oil in turn suggests that either the ^{4}He estimate of an average water residence time of 2 Ma is too low, or a small amount of flow occurs and that channelised oil migration pathways during secondary migration through the Magnus sandstone

aquifer (e.g. England et al., 1987) limits the volume of water that the oil equilibrates with. Within the uncertainty of the absolute derived ^{4}He groundwater dates, we cannot distinguish between these two possibilities.

3.3. Dating groundwater associated with Hugoton-Panhandle giant gas field, Kansas/Texas/Oklahoma, USA

3.3.1. Geological background

The Hugoton-Panhandle giant gas field, located across SW Kansas and the Texas and Oklahoma panhandles in the USA (Fig. 5), is the case type example of high nitrogen (~20%) concentrations in a (CH_4 dominated) natural gas being linked with high helium (~0.6%) concentrations. The principal gas producing zone is from Permian carbonates at between 400 and 900 m depth on the south and western margin of the Anadarko basin. In the Hugoton section of the gas field, a combination of stratigraphy and hydrodynamic trapping are thought to be the main trapping mechanisms in this portion of the field. In the Panhandle section of the field, the Permian structural anticline overlying the Wichita uplift forms the main trapping mechanism in this portion of the field.

3.3.2. Developing ^{4}He model groundwater ages

Ballentine and Sherwood Lollar (2002) studied the noble gases, composition and stable isotope in gas samples from across the gas field and developed a model to describe the role of the groundwater in the collection, transport and focussing of the ^{4}He and ^{4}He-associated nitrogen. In the Hugoton-Panhandle gases, Ballentine and Sherwood Lollar noted that the groundwater-derived noble gases were unfractionated from values found in typical groundwater, suggesting quantitative transfer from the groundwater into the gas phase. In this case, the concentration of a groundwater-derived noble gas, such as ^{20}Ne, in groundwater and the ^{4}He/^{20}Ne ratio measured in the gas phase is all that is required to compute the initial ^{4}He concentrations in the groundwater. See Appendix 3 for detailed calculations. The initial crustal radiogenic ^{4}He concentrations in the groundwater associated with different gas producing wells are listed in Table 1.

Although the Hugoton-Panhandle system has the most straightforward model with which to calculate initial associated-water ^{4}He concentrations, the dimensions of the regional groundwater system that must have contacted the gas field are unconstrained (Ballentine and Sherwood Lollar, 2002). Because the aquifer thickness and porosity is such a fundamental constraint on derived model ^{4}He age, exemplified by the San Juan study above, derived ages can be used with most confidence only in the assessment of change of relative groundwater age across the system. We nevertheless, include this study to exemplify both this particular point and also provide a platform for

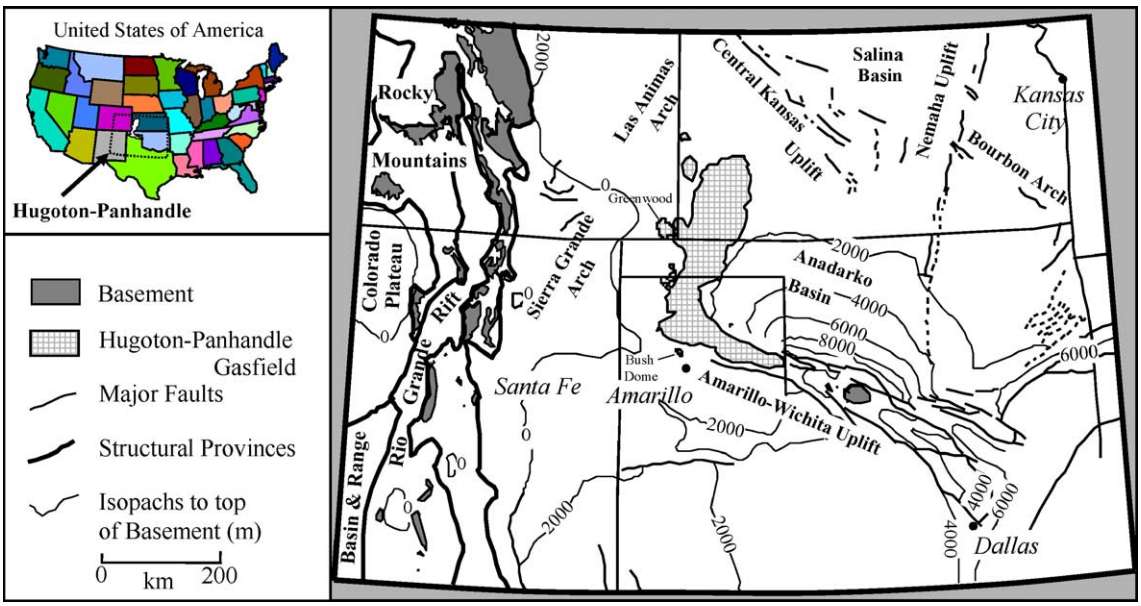

Fig. 5. Hugoton-Panhandle giant gas field and associated major structural features. It is located and extends 350 km across SW Kansas and the Texas and Oklahoma panhandles in the USA. The principle gas-producing zone is from Permian carbonates at between 400 and 900 m depth on the south and western margin of the Anadarko basin (after Ballentine and Sherwood Lollar, 2002).

discussion of the confidence that can be applied to understanding the significance of the variance in ages derived from a single regional system and a discussion of the usefulness of 'absolute' ages even given such large uncertainties.

In a closed system, if we take an average upper crust composition to represent Hugoton-Panhandle reservoir condition, i.e. U concentration 2.8 ppm, Th/U=3.8 and density 2.6 g/cm^3 (Taylor and McLennan, 1985), the porosity is assumed to be 15%. The accumulation of ^{4}He in the groundwater by in situ production can be calculated using Eqs. (2) and (3) as 9.48×10^{-12} cm^3 STP ^{4}He/cm^3 H_2O year. The ages of groundwater associated with the gas reservoir is then obtained. These ages are between 3.53×10^8 and 8.74×10^8 years (Table 1).

A simple mass balance shows that the Hugoton-Panhandle gas reservoir is not a closed system for ^{4}He (Ballentine and Sherwood Lollar, 2002). The recoverable gas content of the Hugoton-Panhandle system is estimated to be 2.3×10^{12} m^3 STP, with an average ^{4}He content of 0.6%. This gives a minimum volume of ^{4}He in the system to be 1.38×10^{10} m^3 STP (^{4}He). When considering two time periods, 300 Ma, representing the time since the Anadarko basin started to form, and 530 Ma, representing the time since the last Mid-Cambrian perturbation of the basement system, the volume of crust required to produce ^{4}He are 202,200 km^3 and 114,500 km^3, respectively. Parameters used in this calculation are the average upper crust composition described above (Table 2). These values can be compared with the sedimentary fill of the Anadarko basin below 2 km depth, estimated to be ~330,000 km^3, and the volume of the crystalline rocks forming the Amarillo uplift, estimated to be ~1400 km^3 (Ballentine and Sherwood Lollar, 2002). This simple mass balance demonstrates that the uplifted crystalline basement beneath the system is two orders of magnitude too small to account for the observed ^{4}He. It also suggests that an external flux of ^{4}He is required to explain the ^{4}He concentration in the groundwater. Again, with ^{3}He/^{4}He ratios of between $0.14R_a$ and $0.25R_a$, a resolvable magmatic contribution to the He is also required, providing further evidence of a deep volatile contribution to this system.

Although we have used the Anadarko basin for comparison, unlike the hydrocarbons which for source maturity reasons are most probably sourced from this basin complex, there is no reason for the radiogenic noble gas source to be restricted to this geographical location. Therefore, the ^{4}He accumulation in the groundwater is the sum of ^{4}He produced by in situ production and ^{4}He from the external flux. The external crustal flux is calculated using Eqs. (4) and (5) as in the San Juan Basin and Magnus oilfield cases above. The porosity and thickness of the aquifer which contacts Hugoton-Panhandle gas reservoir are arbitrarily taken to be 15% and 100 m. Other parameters are summarized in Table 2. Again, the ^{4}He accumulation rate in the groundwater by external flux is much higher than that by in situ production. It is the dominant part of the ^{4}He accumulation rate in the groundwater in an open system, which for these parameters is calculated to be 1.54×10^{-9} cm^3 STP ^{4}He/cm^3 H_2O year. The model ages of groundwater associated with Hugoton-Panhandle gas field then are calculated to be between 2.16×10^6 and 5.35×10^6 years (Table 1; Fig. 6). Although the samples are located along a north–south traverse of the Hugoton-Panhandle field up to 200 km from the south of the reservoir, the calculated initial ^{4}He concentrations in the groundwater and then the groundwater ages are scattered and show no spatial trend from the south to the north. When taking into account the uncertainties of ^{4}He in the measurements, the calculation of initial ^{4}He in the groundwater and the parameters used in calculation, we argue that they are within error of each other. This is probably because the direction of the

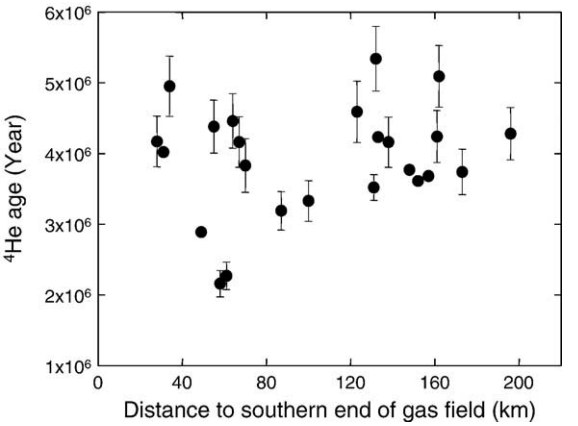

Fig. 6. ^{4}He ages of groundwater associated with Hugoton-Panhandle giant gas field, USA (errors only include the uncertainties of ^{4}He in the measurements and calculation of initial ^{4}He in the groundwater). Although these dates are scattered to some extent they are within the errors of each other if we take all uncertainties into account. There is no clear spatial trend of these ages along the water flow direction from the west to the east of the gas field. These dates suggest there is no significant preservation of formation water during reservoir filling and seal. The groundwater contacting the reservoir over 320 km length is similar in age. The groundwater ages of ~4 Ma is the time required for the accumulation of N_2 and ^{4}He before transport, interaction and degassing into the gas reservoir.

inferred groundwater flow is from the west to the east (Larson, 1971) and these samples are at a similar stage along the groundwater flow path.

3.3.3. Hugoton-Panhandle gas field—discussion and summary

Before we discuss the usefulness of our ^{4}He groundwater ages, we need to consider the timing of the major geological events of Hugoton-Panhandle gas field. The erosion and basin filling started pre-Pennsylvanian and continued until the Permian (~300 Ma). The seal for the hydrocarbon reservoir formed in the late Permian (~250 Ma) (Parham and Campbell, 1993), with almost contemporaneous onset of hydrocarbon oil and gas generation in the Anadarko basin (Schmoker, 1986). Because the ^{4}He groundwater ages are within error of each other, we consider the average model ^{4}He groundwater age of ~4 Ma. This is far younger than the age of reservoir formation and filling of the hydrocarbon gases. Even with extreme uncertainties, it is unlikely that these groundwater ages can be more than 100 Ma and similarly is unlikely to be young water. These groundwater dates suggest that there is no significant preservation of formation water.

The gases present in the reservoir are a mixture from two sources. One is derived from groundwater which contains air-derived and crustal radiogenic noble gases (including high concentrations of ^{4}He) as well as nitrogen with a distinct isotopic composition, the other source has supplied CH_4 and N_2 without a significant groundwater contact (Ballentine and Sherwood Lollar, 2002). The model proposed by Ballentine and Sherwood Lollar requires the groundwater containing the dissolved 'groundwater-derived' gases to contact an established gas reservoir, whereupon equilibration between the gas and water causes almost quantitative transfer of the dissolved gasses into the gas phase. This groundwater, although with considerable uncertainty must have ^{4}He accumulation ages on the order of millions of years (here ~4 Ma) to accumulate the ^{4}He (and N_2) before transport, interaction and degassing into the gas reservoir to form a commercially viable ^{4}He gas deposit. We can speculate that ~4 Myr old groundwater was driven eastwards to contact the established gas field by tectonic uplift to the west of the system. This could have been one of a number of events in this tectonically active portion of the US. At our current level of understanding of the process that produce ^{4}He and N_2 in reservoirs, even this crude date information is important to place some constrain on the regional parameter, groundwater age, which plays the dominant role in controlling when and how commercial ^{4}He occurrences are formed.

4. Summary

We show, using three case studies, how the ^{4}He concentration of groundwater in contact with a hydrocarbon phase can be estimated from the noble gas systematics of the hydrocarbon phase. This is dependant on identifying a physical model that accounts for noble gas concentrations and fractionation from end-member compositions, already established for these cases. The Panhandle giant gas field (Texas, Oklahoma, Kansas) and the San Juan coal gas field (New Mexico) case studies illustrate different gas/water interaction. These show quantitative transferral of dissolved gases into the sampled gas phase and an open system degassing behaviour of the source groundwater, respectively. The third case study, the Magnus oilfield, shows oil/water equilibrium between phases.

The source of the ^{4}He in the hydrocarbon-associated groundwater is due to a time-dependant accumulation process. In all studies ^{4}He produced by radioactive decay of U and Th within the aquifer itself cannot account for the concentration of ^{4}He in the hydrocarbon-associated groundwater, requiring a flux from depth. ^{3}He/^{4}He ratios in all studies indicate a small magmatic contribution reinforcing this conclusion. The assumption of an average crustal flux based on the steady state production of ^{4}He in the continental crust is the single most unconstrained value used in these estimates. In spite of uncertainty of the local ^{4}He flux, we show from the case studies how a unique insight into the different systems is nevertheless possible with these hydrocarbon phase-derived ^{4}He ages of the associated groundwater.

Acknowledgements

This research has been supported by the Swiss National Science Foundation. Eddie Pippin from Burlington Resources, Farmington, USA, kindly provided sampling assistance, production, hydrogeological and background information on the hydrocarbon reservoirs. This work has benefited much from discussions with Rolf Kipfer, Ingo Leya, Werner Aeschbach-Hertig and support from Rainer Wieler and Alex Halliday. ZZ especially thanks Heinrich Baur for the assistance in the laboratory. We thank Maria Clara Castro and Justin Kulongoski for their helpful and positive reviews. Editorial handling of this manuscript by David Hilton is very much appreciated. [**SLG**]

Appendix 1. Calculation of the initial ^{4}He in the groundwater associated with the San Juan Basin coalbed methane gas field, New Mexico/Colorado, USA

The noble gas data from The San Juan Basin gas wells show that ^{3}He/^{4}He and ^{40}Ar/^{36}Ar ratios are all distinct from air ratios. Since measured ^{4}He/^{20}Ne ratios range between 854 and 28,200 compared with the atmospheric ratio of 0.288 in the groundwater this indicates that atmosphere-derived ^{4}He contributions are negligible in all cases. This also suggests that the ^{3}He/^{4}He ratios above crustal production values are due to a resolvable mantle He contribution to the San Juan gases. It is nevertheless necessary for completeness to correct any measured He isotopic composition for air-derived contributions by using the observed air-derived ^{20}Ne concentration following (Craig et al., 1978):

$$\left(^3\mathrm{He}/^4\mathrm{He}\right)_c = \frac{\left(^3\mathrm{He}/^4\mathrm{He}\right)_s \times \left(^4\mathrm{He}/^{20}\mathrm{Ne}\right)_s/\left(^4\mathrm{He}/^{20}\mathrm{Ne}\right)_{air} - \left(^3\mathrm{He}/^4\mathrm{He}\right)_{air}}{\left(^4\mathrm{He}/^{20}\mathrm{Ne}\right)_s/\left(^4\mathrm{He}/^{20}\mathrm{Ne}\right)_{air} - 1} \quad (6)$$

where: subscripts c, s and air refer to the corrected, measured and air-derived ratios, respectively. After this correction $(^3\mathrm{He}/^4\mathrm{He})_c \approx (^3\mathrm{He}/^4\mathrm{He})_s$ in San Juan Basin gas samples.

Once atmosphere-derived He is subtracted, the ^{3}He/^{4}He ratio represents the sum of only two components, the crust and the mantle. The contribution of crust ^{4}He is then given by (Ballentine et al., 2002):

$$[^4\mathrm{He}]_{crust} = \frac{[^4\mathrm{He}]_{total} \times [(^3\mathrm{He}/^4\mathrm{He})_{mantle} - (^3\mathrm{He}/^4\mathrm{He})_c]}{[(^3\mathrm{He}/^4\mathrm{He})_{mantle} - (^3\mathrm{He}/^4\mathrm{He})_{crust}]} \quad (7)$$

where: subscripts mantle, crust and c refer to the mantle, crust and air-corrected values. If it is assumed that $R/R_a = 6.0$ and 0.007 (Dunai and Porcelli, 2002) for mantle and crustal radiogenic sources, respectively, then the percentage crustal radiogenic ^{4}He in San Juan gas samples varies between 94% and 99%. The resolved crustal radiogenic ^{4}He concentrations in these samples are shown in Table 1. A resolvable magmatic He component in all samples requires a deep crustal He flux from beneath the basin.

^{40}Ar/^{36}Ar ratios greater than air are due to a resolvable crustal-radiogenic ^{40}Ar* component. The ^{40}Ar* can be resolved by using equation following Ballentine et al. (2002):

$$[^{40}\mathrm{Ar}^*] = [^{40}\mathrm{Ar}]_{total} \times [1 - (^{40}\mathrm{Ar}/^{36}\mathrm{Ar})_{air}/(^{40}\mathrm{Ar}/^{36}\mathrm{Ar})_s] \quad (8)$$

where: subscripts total refer to the total concentration, air and s refer to the isotopic composition of the atmosphere (Ozima and Podosek, 1983) and sample, respectively.

Both water derived noble gas ^{20}Ne/^{36}Ar ratios and radiogenic ^{4}He/^{40}Ar* ratios in all samples show a clear fractionation trend that is consistent with a gas/groundwater phase partition process. The observation that both radiogenic and water derived species are coherently fractionated indicates that these differently sourced noble gases are premixed before the fractionating event, probably in the groundwater (e.g. Ballentine and Sherwood Lollar, 2002). This process can be modelled by a Rayleigh fractionation of noble gases in the groundwater exsolving into the gas phase (Zhou et al., in press). This Rayleigh fractionation of noble gas exolving from groundwater into gas phase allows us to calculate the initial crustal radiogenic ^{4}He in the groundwater phase.

Assuming equilibrium of noble gases between gas and groundwater phase at each degassing stage, we can calculate ^{4}He/^{36}Ar and ^{20}Ne/^{36}Ar ratios in the groundwater using the measured ^{4}He/^{36}Ar ratios and ^{20}Ne/^{36}Ar in the gas phase (Ballentine et al., 2002):

$$\left(\frac{A}{B}\right)_{groundwater} = \left(\frac{A}{B}\right)_{gas} / \alpha \quad (9)$$

$$\alpha = \frac{\frac{r_A}{\varphi_A} K_A^{groundwater}}{\frac{r_B}{\varphi_B} K_B^{groundwater}}$$

where:

$\left(\frac{A}{B}\right)_{groundwater}$	A/B ratio in the groundwater and A and B are different noble gases
$\left(\frac{A}{B}\right)_{gas}$	A/B ratio in the gas phase
α	Fractionation coefficient given for gas/groundwater system
K_A, K_B	Henry's constants for gases A and B
r_A, r_B	Groundwater phase activity coefficients
φ_A, φ_B	Gas phase fugacity coefficients

Based on Rayleigh fractionation law:

$$\left(\frac{A}{B}\right)_{groundwater} = \left(\frac{A}{B}\right)_0 f^{\alpha-1} \quad (10)$$

where:

$\left(\frac{A}{B}\right)_0$	The original groundwater phase A/B ratio
f	Fraction of B remaining in the groundwater phase

The fraction of ^{36}Ar remaining in the groundwater can be calculated. In the San Juan Basin study, initial ^{36}Ar concentrations and $^{20}Ne/^{36}Ar$ ratios in the air saturated water (ASW) are determined following Henry's law corrected for an altitude of 600 m, a recharge temperature of 10 °C and an unfractionated excess air component assuming 15% excess air Ne (e.g. Stute et al., 1992, 1995; Kipfer et al., 2002). The value of $^{20}Ne/^{36}Ar$ is 0.156.

Combined with the initial ^{36}Ar concentration calculated above, which is 1.09×10^{-6} cm^3 STP/g H_2O, the fraction of ^{36}Ar remaining in the groundwater phase and the present $^4He/^{36}Ar$ in the groundwater, the initial $^4He/^{36}Ar$ in the groundwater can be calculated, then the initial ^4He concentrations in the groundwater obtained (Table 1). These initial ^4He concentrations in the groundwater are only derived from the crust, the mechanism can be accumulation of ^4He in situ production in a closed system, or ^4He in situ production combined with an external ^4He flux in an open system.

Appendix 2. Calculation of the initial ^4He concentrations in the groundwater associated with Magnus oilfield, North Sea, UK

Ballentine et al. (1996) studied the noble gases in the Magnus oilfield. Measured data are shown in Table 1. $^3He/^4He$ ratios differ significantly from the north of the field, which has a value of $0.2R_a$, to the south of the field, which has a value of $0.38R_a$. High $^3He/^4He$ provides unambiguous identification of a mantle-derived noble gas component in these samples. If it is assumed that radiogenic and mantle end member values of $^3He/^4He$ are $0.02R_a$ and $8.0R_a$, respectively, then the values correspond to a mantle ^4He contribution of between 2.3 and 4.5% of the total ^4He present. In all samples, $^4He/^{20}Ne$ ratios exceed 7300, which compares with the air value of 0.288. Air derived helium contributions are, therefore, negligible, and the measured ratio can be considered to represent a two component mixture of mantle-derived and radiogenic helium.

Atmosphere-derived ^{20}Ne and ^{36}Ar in the Magnus oil have been due to noble gas partitioning between a seawater derived groundwater and the oil phase. It should be noted that there is no gas phase present in the Magnus field. Seawater in equilibrium with air contains 1.47×10^{-7} cm^3 STP ^{20}Ne/cm^3 H_2O and 7.65×10^{-7} cm^3 STP ^{36}Ar/cm^3 H_2O, respectively. Using a temperature of 373 K, seawater salinity of 0.623 M NaCl equivalent for reservoir conditions, the solubility of Ne and Ar is taken to be 2517 and 1407 kg atm/mol, the measured ^{20}Ne and ^{36}Ar oil concentrations are $1.22(\pm0.18)\times10^{-6}$ cm^3 STP ^{20}Ne/cm^3 Oil and $6.79(\pm0.21)\times10^{-6}$ cm^3 STP ^{36}Ar/cm^3 Oil, respectively. These values define an oil and water volume ratio for the Magnus system of $V_{oil}/V_{water}=0.009\pm0.003$ (Ballentine et al., 1996). In this calculation, one sample (A1) was excluded on the basis that it was unrepresentative of the bulk of the Magnus oil and had probably mixed with meteoric water. We do not take this sample into account in our study.

The calculation of in situ radiogenic ^4He production in the Magnus reservoir showed that it can only account for 9–21% of the radiogenic ^4He now trapped within it. As discussed before, the mass balance of atmosphere-derived noble gases now within the Magnus oil can only reasonably be accounted for by partitioning of noble gases between the groundwater and oil phase. Because the major portion of the radiogenic noble gases cannot be sourced in situ, it is reasonable to assume that the radiogenic noble gases were also partitioned between the groundwater and oil phase.

The resolved crustal radiogenic ^4He concentrations in Magnus oil samples, using Eqs. (6) and (7), are shown in Table 1. Under reservoir conditions (Temperature 373 K, seawater salinity 0.623 M NaCl equivalent), if we take $V_{oil}/V_{gas}=0.009$, solubility of He in the oil is the same as Ne (e.g. Kharaka and Specht, 1988), which is 2517 kg atm/mol, solubility of Ar in the oil is 1407 kg atm/mol, solubility of He and Ar in the seawater as 2199 and 1406 kg atm/mol, respectively, the initial $^4He/^{36}Ar$ ratios in the groundwater before water/oil partition of noble gases can be calculated using the following equation (Ballentine et al., 2002):

$$\left(\frac{^4He}{^{36}Ar}\right)_{initial}=\left(\frac{^4He}{^{36}Ar}\right)_{oil}\frac{\left(\frac{V_{oil}}{V_{water}}+\frac{K_{He(oil)}}{K_{He(water)}}\right)}{\left(\frac{V_{oil}}{V_{water}}+\frac{K_{Ar(oil)}}{K_{Ar(water)}}\right)} \quad (11)$$

Where:

$(^4He/^{36}Ar)_{initial}$ Initial $^4He/^{36}Ar$ ratio in the groundwater
$(^4He/^{36}Ar)_{oil}$ $^4He/^{36}Ar$ ratio in the oil phase
V_{oil}, V_{water} Volumes of oil and groundwater in contact
$K_{He(oil)}$, $K_{He(water)}$ Solubilities of He in oil and groundwater
$K_{Ar(oil)}$, $K_{Ar(water)}$ Solubilities of Ar in oil and water

^{36}Ar is mainly derived from the air dissolved into the groundwater. Seawater in equilibrium with air contains

7.65×10^{-7} cm^3 STP ^{36}Ar/cm^3 H_2O. The initial crustal radiogenic ^{4}He in the groundwater can then be calculated (Table 1).

Appendix 3. Calculation of the initial ^{4}He concentrations in the groundwater associated with Hugoton-Panhandle Giant Gas Field, Kansas/Texas/Oklahoma, USA

Ballentine and Sherwood Lollar (2002) studied the noble gases, composition and stable isotope in the gas samples from the gas field. The ^{3}He/^{4}He is reasonably uniform throughout the Hugoton-Panhandle gas system, varying between 0.14 and $0.25R_a$. High ^{4}He/^{20}Ne (>18,000) relative to air (0.288) means that atmosphere He contributions are negligible. Assuming a crustal radiogenic ^{3}He/^{4}He end-member of $0.02R_a$ and a mantle ^{3}He/^{4}He end member of $8R_a$, the ^{3}He/^{4}He ratios indicate that between 1.5% and 2.9% of the ^{4}He is mantle-derived, and the remainder crustal-radiogenic. The clear relationship between crustal radiogenic ^{4}He and groundwater-derived ^{20}Ne suggests that the crustal ^{4}He and groundwater-derived ^{20}Ne ratio must have been established before mixing and variable dilution with the dominant hydrocarbon phase. ^{20}Ne/^{36}Ar in the gas phase are identical to predicted values for meteoric water and indicate little or no fractionation, and therefore an efficient degassing process. A correlation between ^{20}Ne/N_2 and ^{4}He/N_2 is interpreted as two-component mixing between a ^{4}He- and ^{20}Ne-associated N_2 end member and a nitrogen component that contains neither ^{4}He nor ^{20}Ne. The physical model developed for the timing and mechanism of hydrocarbon, N_2 and He-associated N_2 mixing is that groundwater degassing occurs when migrating and undegassed water contacts and equilibrates with an existing gas phase in the Hugoton-Panhandle reservoir.

Based on the model described above and the evidence that an efficient degassing occurred between gas and groundwater phase, the measured ^{4}He/^{20}Ne ratios in the gas phase represent the initial ^{4}He/^{20}Ne ratios in the groundwater phase. ^{20}Ne is mainly derived from air dissolved in the groundwater, it is a function of temperature, excess air and recharge temperature. If we estimate these parameters to be 10 °C, 10% excess air Ne and 1000 m, respectively, the ^{20}Ne concentration in groundwater is 1.8×10^{-7} cm^3 STP ^{20}Ne/cm^3 H_2O. After correcting ^{4}He concentrations in the gas phase with air and mantle-derived components, the initial crustal radiogenic ^{4}He in the groundwater can be calculated (Table 1).

References

Andrews, J.N., 1985. The isotopic composition of radiogenic helium and its use to study groundwater movement in confined aquifers. Chem. Geol. 49, 339–351.

Ballentine, C.J., Burnard, P.G., 2002. Production, release and transport of noble gases in the continental crust. Rev. Mineral. Geochem. 47, 481–538.

Ballentine, C.J., Sherwood Lollar, B., 2002. Regional groundwater focusing of nitrogen and noble gases into the Hugoton-Panhandle giant gas field, USA. Geochim. Cosmochim. Acta 66, 2483–2497.

Ballentine, C.J., O'Nions, R.K., Oxburgh, E.R., Horvath, F., Deak, J., 1991. Rare gas constraints on hydrocarbon accumulation, crustal degassing and groundwater flow in the Pannonian Basin. Earth Planet. Sci. Lett. 105, 229–246.

Ballentine, C.J., Mazurek, M., Gautschi, A., 1994. Thermal constraints on crustal rare gas release and migration: evidence from Alpine fluid inclusions. Geochim. Cosmochim. Acta 58, 4333–4348.

Ballentine, C.J., O'Nions, R.K., Coleman, M.L., 1996. A Magnus opus: helium, neon, and argon isotopes in a North Sea oilfield. Geochim. Cosmochim. Acta 60, 831–849.

Ballentine, C.J., Burgess, R., Marty, B., 2002. Tracing fluid origin, transport and interaction in the crust. Rev. Mineral. Geochem. 47, 539–614.

Bethke, C.M., Zhao, X., Torgersen, T., 1999. Groundwater flow and the ^{4}He distribution in the Great Artesian Basin of Australia. J. Geophys. Res. 104, 12999–13011.

Castro, M.C., 2004. Helium sources in passive margin aquifers—new evidence for a significant mantle ^{3}He source in aquifers with unexpectedly low in situ ^{3}He/^{4}He production. Earth Planet. Sci. Lett. 222, 897–913.

Castro, M.C., Jambon, A., de Marsily, G., Schlosser, P., 1998a. Noble gases as natural tracers of water circulation in the Paris Basin 1. Measurements and discussion of their origin and mechanisms of vertical transport in the basin. Water Resour. Res. 34, 2443–2466.

Castro, M.C., Goblet, P., Ledoux, E., Violett, S., de Marsily, G., 1998b. Noble gases as natural tracers of water circulation in the Paris Basin 2. Calibration of a groundwater flow model using noble gas isotope data. Water Resour. Res. 34, 2467–2483.

Collon, P., Kutschera, W., Loosli, H.H., Lehmann, B.E., Purtschert, R., Love, A., Sampson, L., Anthony, D., Cole, D., Davids, B., Morrissey, D.J., Sherrill, B.M., Steiner, M., Pardo, R.C., Paul, M., 2000. ^{81}Kr in the Great Artesian Basin, Australia: a new method for dating very old groundwater. Earth Planet. Sci. Lett. 182, 103–113.

Colwell, F.S., Onstott, T.C., Delwiche, M.E., Chandler, D., Fredrickson, J.K., Yao, Q.-J., McKinley, J.P., Boone, D.R., Griffiths, R., Phelps, T.J., Ringelberg, D., White, D.C., LaFreniere, L., Balkwill, D., Lehman, R.M., Konosky, J., Long, P.E., 1997. Microorganisms from deep, high temperature sandstones: constraints on microbial colonization. FEMS Microbiol. Rev. 20, 425–435.

Craig, H., Lupton, J.E., 1976. Primordial neon, helium, and hydrogen in oceanic basalts. Earth Planet. Sci. Lett. 31, 369–385.

Craig, H., Lupton, J.E., Horib, Yo., 1978. A mantle helium component in circum Pacific volcanic gases: Hakone, the Marianas, and Mt. Lassen. In: Alexander, E.C., Ozima, M. (Eds.), Terrestrial Rare Gases. Japan Sci. Societies Press, Tokyo, pp. 3–16.

Dunai, T.J., Porcelli, D., 2002. Storage and transport of noble gases in the subcontinental lithosphere. Rev. Mineral. Geochem. 47, 371–409.

Emery, D., Smalley, P.C., Oxtoby, N.H., 1993. Synchronous oil migration and cementation in sandstone reservoirs demonstrated

by quantitative description of diagenesis. Philos. Trans. R. Soc. Lond. Ser. A: Math. Phys. Eng. Sci. 344, 115–125.
England, W.A., Mackenzie, A.J., Mann, M.N., Quigley, T.M., 1987. The movement and entrapment of fluids in the subsurface. J. Geol. Soc. (Lond.) 144, 327–347.
Fabryka-Martin, J., Davis, S.N., Elmore, D., 1987. Applications of ^{129}I and ^{36}Cl to hydrology. Nucl. Instrum. Methods Phys. Res., B Beam Interact. Mater. Atoms 29, 361–371.
Farley, K.A., 2002. (U–Th)/He dating: techniques, calibrations, and applications. Rev. Mineral. Geochem. 47, 819–845.
Finkelman, R.B., Oman, C.L., Bragg, L.J., Tewalt, S.J., 1994. The U. S. Geological Survey Coal Quality Data Base (COALQUAL). Open-File Report 94-177. United States Department of the Interior Geological Survey.
Fontes, J.C., Garnier, J.M., 1979. Determination of the initial ^{14}C activity of total dissolved carbon: a review of existing models and a new approach. Water Resour. Res. 15, 399–413.
Heaton, T.H.E., 1984. Rates and sources of ^{4}He accumulation in groundwater. Hydrol. Sci. J. 29, 29–47.
Heydari, E., 2000. Porosity loss, fluid flow, and mass transfer in limestone reservoirs: application to the Upper Jurassic Smackover Formation, Mississippi. AAPG Bull. 84, 100–118.
Hoehn, E., von Gunten, H.R., 1989. Radon in ground water: a tool to assess infiltration from surface waters to aquifers. Water Resour. Res. 25, 1795–1803.
Horstad, I., Larter, S.R., Mills, N., 1992. A quantitative model of biological petroleum degradation within the Brent Group reservoir in the Gullfaks field, Norwegian North Sea. Org. Geochem. 19, 107–117.
Kharaka, Y.K., Specht, D.J., 1988. The solubility of noble gases in crude oil at 25–100 °C. Appl. Geochem. 3, 137–144.
Kipfer, R., Aeschbach-Hertig, W., Peeters, F., Stute, M., 2002. Noble gases in lakes and ground waters. Rev. Mineral. Geochem. 47, 615–700.
Lafargue, E., Barker, C., 1988. Effect of water washing on crude-oil compositions. AAPG Bull. 72, 263–276.
Larson, T.G., 1971. Hydrodynamic interpretation of mid continent. In: Adler, F.J. (Ed.), Future petroleum provinces of the United States: their geology and potential, vol. 2. American Association of Petroleum Geologists, Tulsa, OK, pp. 1043–1046.
Lehmann, B.E., Love, A., Purtschert, R., Collon, P., Loosli, H.H., Kutschera, W., Beyerle, U., Aeschbach-Hertig, W., Kipfer, R., Frape, S., Herczeg, A.L., Moran, J., Tolstikhin, I.N., Groning, M., 2003. A comparison of groundwater dating with Kr-81, Cl-36 and He-4 in four wells of the Great Artesian Basin, Australia. Earth Planet. Sci. Lett. 211, 237–250.
Lippolt, H.J., Weigel, E., 1988. ^{4}He diffusion in ^{40}Ar retentive minerals. Geochim. Cosmochim. Acta 52, 1449–1458.
Loosli, H.H., 1983. A dating method with ^{39}Ar. Earth Planet. Sci. Lett. 63, 51–62.
Lynch, F.L., 1996. Mineral interaction, fluid flow, and Frio sandstone diagenesis: evidence from the rocks. AAPG Bull. 80, 486–504.
Martini, A.M., Budai, J.M., Walter, L.M., Schoell, M., 1996. Microbial generation of economic accumulations of methane within a shallow organic-rich shale. Nature 383, 155–158.
Martini, A.M., Walter, L.M., Budai, J.M., Ku, T.C.W., Kaiser, C.J., Schoell, M., 1998. Genetic and temporal relations between formation waters and biogenic methane: Upper Devonian Antrim Shale, Michigan Basin, USA. Geochim. Cosmochim. Acta 62, 1699–1720.
Marty, B., Torgersen, T., Meynier, V., O'Nions, R.K., de Marsily, G., 1993. Helium isotope fluxes and groundwater ages in the Dogger Aquifer, Paris basin. Water Resour. Res. 29, 1025–1035.
Marty, B., Dewonck, S., France-Lanord, C., 2003. Geochemical evidence for efficient aquifer isolation over geological timeframes. Nature 425, 55–58.
Mavor, M.J., Close, J.C., Pratt, T.J., 1991. Western Cretaceous coal seam project summary of the Completion Optimization and Assessment Laboratory (COAL) site. Gas Research Institute Topical Report GRI-91/0377.
Osenbrück, K., Lippmann, J., Sonntag, C., 1998. Dating very old pore waters in impermeable rocks by noble gas isotopes. Geochim. Cosmochim. Acta 62, 3041–3045.
Ozima, M., Podosek, F.A., 1983. Noble Gas Geochemistry. Cambridge Univ. Press, Cambridge.
Parham, K.D., Campbell, J.A., 1993. Wolfcampian shallow shelf carbonate–Hugoton embayment, Kansas and Oklahoma. In: Bebout, D.G., White, W.A., Hentz, T.F. (Eds.), Atlas of Major Midcontinent Gas Reservoirs. Bureau of Economic Geology, University of Texas at Austin, Austin, pp. 9–12.
Patriarche, D., Castro, M.C., Goblet, P., 2004. Large-scale hydraulic conductivities inferred from three-dimensional groundwater flow and ^{4}He transport modelling in the Carrizo aquifer, Texas. J. Geophys. Res. 109, B11202 doi:10.1029/2004JB0031173.
Phillips, F.M., Peeters, L.A., Tansey, M.K., 1986. Paleoclimatic inferences from an isotopic investigation of groundwater in the central San Juan Basin, New Mexico. Quaternary Res. 26, 179–193.
Phillips, F.M., Tansey, M.K., Peeters, L.A., 1989. An isotopic investigation of groundwater in the central San Juan Basin, New Mexico: carbon 14 dating as a basis for numerical flow modelling. Water Resour. Res. 25, 2259–2273.
Pinti, D.L., Marty, B., 1998. The origin of helium in deep sedimentary aquifers and the problem of dating very old groundwater. In: Parnell, J. (Ed.), Dating and Duration of Fluid Flow and Fluid–Rock Interaction. The Geological Society, London, pp. 53–68.
Rueter, P., Rabus, R., Wilkes, H., Aeckersberg, F., Rainey, F.A., Jannasch, H.W., Widdel, F., 1994. Anaerobic oxidation of hydrocarbons in crude oil by new types of sulphate reducing bacteria. Nature 372, 455–458.
Sano, Y., Wakita, H., Huang, C.W., 1986. Helium flux in a continental land area from ^{3}He/^{4}He ration in northern Taiwan. Nature 323, 55–57.
Schmoker, J.W., 1986. Oil generation in the Anadarko basin, Oklahoma and Texas: modelling using Lopatin's method. Oklahoma Geological Survey Special Publication, vol. 86-3. 40 pp.
Scott, A.R., Kaiser, W.R., Walter Jr., B.A., 1994. Thermogenic and secondary biogenic gases, San Juan basin, Colorado and New Mexico—implications for coalbed gas producibility. AAPG Bull. 78, 1186–1209.
Snyder, G.T., Riese, W.C., Franks, S., Fehn, U., Pelzmann, W.L., Gorody, A.W., Moran, J.E., 2003. Origin and history of waters associated with coalbed methane: ^{129}I, ^{36}Cl, and stable isotope results from the Fruitland formation, CO and NM. Geochim. Cosmochim. Acta 67, 4529–4544.
Solomon, D.K., Schiff, S.L., Poreda, R.J., Clarke, W.B., 1993. A validation of the ^{3}H/^{3}He-method for determining ground water recharge. Water Resour. Res. 29, 2951–2962.
Solomon, D.K., Hunt, A., Poreda, R.J., 1996. Source of radiogenic helium-4 in shallow aquifers: implications for dating young ground water. Water Resour. Res. 32, 1805–1813.
Stone, W.J., Lyford, F.P., Frenzel, P.F., Mizell, N.H., Padgett, E.T., 1983. Hydrogeology and water resources of San Juan Basin, New Mexico. Hydrologic Report, vol. 6. New Mexico Bureau of Mines and Mineral Resources.

Stute, M., Sonntag, C., Deak, J., Schlosser, P., 1992. Helium in deep circulating groundwater in the Great Hungarian plain: flow dynamics and crustal and mantle helium fluxes. Geochim. Cosmochim. Acta 56, 2051–2067.

Stute, M., Clark, J.F., Schlosser, P., Broecker, S., Bonani, G., 1995. A 30,000 yr continental paleotemperature record derived from noble gases dissolved in groundwater from the San Juan Basin, New Mexico. Quat. Res. 43, 209–220.

Summa, L.L., 1995. Diagenesis and reservoir quality prediction. Rev. Geophys. 33, 87–94.

Takahata, N., Sano, Y., 2000. Helium flux from a sedimentary basin. Appl. Radiat. Isotopes 52, 985–992.

Taylor, S.R., McLennan, S.M., 1985. The Continental Crust: Its Composition and Evolution. Blackwell Scientific, Oxford.

Tolstikhin, I., Lehmann, B.E., Loosli, H.H., Gautschi, A., 1996. Helium and argon isotopes in rocks, minerals, and related groundwaters: a case study in northern Switzerland. Geochim. Cosmochim. Acta 60, 1497–1514.

Torgersen, T., 1980. Controls on pore-fluid concentration of ^{4}He and ^{222}Rn and the calculation of $^{4}He/^{222}Rn$ ages. J. Geochem. Explor. 13, 57–75.

Torgersen, T., 1989. Terrestrial helium degassing fluxes and the atmospheric helium budget: implications with respect to the degassing processes of continental crust. Chem. Geol. 79, 1–14.

Torgersen, T., Clarke, W.B., 1985. Helium accumulation in groundwater: I. An evaluation of sources and the continental flux of crustal ^{4}He in the Great Artesian Basin, Australia. Geochim. Cosmochim. Acta 49, 1211–1218.

Torgersen, T., Ivey, G.N., 1985. Helium accumulation in groundwater: II. A model for the accumulation of the crustal ^{4}He degassing flux. Geochim. Cosmochim. Acta 49, 2445–2452.

Torgersen, T., Clarke, W.B., 1987. Helium accumulation in groundwater: III. Limits on helium transfer across the mantle–crust boundary beneath Australia and the magnitude of mantle degassing. Earth Planet. Sci. Lett. 84, 345–355.

Torgersen, T., Habermehl, M.A., Clarke, W.B., 1992. Crustal helium fluxes and heat flow in the Great Artesian Basin, Australia. Chem. Geol. 102, 139–153.

Toth, J., Corbett, T.-W., 1986. Post-Paleocene evolution of regional groundwater flow-system and their relation to petroleum accumulations, Taber area, Southern Alberta, Canada. Bull. Can. Pet. Geol. 34, 339–363.

Tseng, H.Y., Onstott, T.C., 1997. A tectonic origin for the deep subsurface micro organisms of Taylorsville Basin: thermal and fluid flow model constraints. FEMS Microbiol. Rev. 20, 391–397.

Walvoord, M.A., Pelgram, P., Phillips, P.P., Person, M., Kieft, T.L., Fredrickson, J.K., McKinley, J.P., Swenson, J.B., 1999. Groundwater flow and geochemistry in the southeastern San Juan Basin: implications for microbial transport and activity. Water Resour. Res. 35, 1409–1424.

Ward, R.C., Robinson, M., 2000. Principles of Hydrology, 4th ed. McGraw-Hill.

Weise, S., Eichinger, L., Forster, M., Salvamoser, J., 1992. Helium-3 and krypton-85 dating of shallow groundwaters: diffusive loss and correlated problems. Isotopes of Noble Gases as Tracers in Environmental Studies. IAEA, Vienna, pp. 147–162.

Winckler, G., Suess, E., Wallmann, K., deLange, G.J., Westbrook, G. K., Bayer, R., 1997. Excess helium and argon of radiogenic origin in Mediterranean brine basins. Earth Planet. Sci. Lett. 15, 225–231.

Zengler, K., Richnow, H.H., Rossello-Mora, R., Michaelis, W., Widdel, F., 1999. Methane formation from long-chain alkanes by anaerobic micro organisms. Nature 401, 266–269.

Zhou, Z., Ballentine, C.J., Kipfer, R., Schoell, M., Thibodeaux, S., in press. Noble gas tracing of groundwater/coalbed methane interaction in the San Juan Basin, USA. Geochim. Cosmochim. Acta.